

# Crystal Structure of Eucaryotic E3, Lipoamide Dehydrogenase from Yeast<sup>1</sup>

Tomohiko Toyoda,\* Kaoru Suzuki,<sup>†</sup> Takeshi Sekiguchi,<sup>†</sup> Lester J. Reed,<sup>‡</sup> and Akio Takenaka\*<sup>2</sup>

\*Department of Life Science, Faculty of Bioscience and Biotechnology, Tokyo Institute of Technology, Yokohama 226-8501; <sup>†</sup>Department of Fundamental Science, Faculty of Science and Technology, Iwaki Meisei University, Fukushima 970-8551; and <sup>‡</sup>Biochemical Institute, The University of Texas at Austin, Austin, Texas 78712-1096, USA

Received for publication, October 27, 1997

The crystal structure of eucaryotic lipoamide dehydrogenase from yeast has been determined by an X-ray analysis at 2.7 (partially at 2.4) Å resolution. The enzyme has two identical subunits related by a pseudo twofold symmetry. The tertiary structure is similar to those of other procaryotic enzymes. The active site, consisting of FAD, Cys44, and Cys49 from one subunit and His457' from the other subunit, is highly conserved. This enzyme is directly bound to the core protein E2 of the 2-oxoglutarate dehydrogenase complex, whereas it is bound to the pyruvate dehydrogenase complex through a protein X. The calculated electrostatic potential suggests two characteristic regions for binding with these two proteins.

**Key words:** crystal structure, lipoamide dehydrogenase, 2-oxoglutarate dehydrogenase complex, pyruvate dehydrogenase complex, X-ray analysis.

The dihydrolipoamide (lipoamide) dehydrogenases are widely known as the E3 component of the pyruvate (PDC), 2-oxoglutarate (OGDC), and branched-chain 2-oxoacid (BCDC) dehydrogenase multienzymatic complexes (1-3). The architecture of the complexes is composed of multiple copies of E1, E2 and E3.<sup>3</sup> The former two enzymes, E1 and E2, are different among the three complexes corresponding to their respective substrates mentioned above, but the E3 enzyme is a common component among them, which catalyzes the oxidation reaction of dihydrolipoyl group attached to the lysine residue of E2 (1). The E2 components form the structural core of the complex. OGDCs in all

organisms and PDCs in Gram-negative bacteria have a similar core with twenty-four copies of E2 packed with the 432 symmetry. The cores of PDCs in procaryotic Gram-positive bacteria (4) and eucaryotes exhibit 532 symmetry and contain sixty copies of E2. In other words, E3s in the latter organisms are incorporated into both cores with 432 and 532 symmetries.

More strictly speaking, in procaryotes, E3 binds the E3 binding domain (E3BD) of E2 directly even in different architectures. In eucaryotes, however, E3 binds E2 directly in OGDC in a similar way (1-3), but for PDC another component X (5-7) is required to incorporate E3 into the E2 core.<sup>4</sup> E3 binds E3BD of X (8), instead of E2, and then X binds E2 (8). This difference suggests that the procaryotic E3 has one face to bind to E2 only, while the eucaryotic E3 has regions for binding the two kinds of proteins, E2 and X.

The tertiary structures of various components have been elucidated: E3BD of OGDC from *Escherichia coli* (9), the lipoyl domains of E2 of PDC from *Bacillus stearothermophilus* (10) and from *E. coli* (11), E3:E3BD complex of PDC from *B. stearothermophilus* (12), the cubic E2 core of PDC from *Azotobacter vinelandii* (13), and E3s from *A. vinelandii* (14), from *Pseudomonas putida* (15), and from *Pseudomonas fluorescens* (16). These are all from procaryotic systems. On the other hand, the three-dimensional structures of eucaryotic E3s have not yet been reported, though a low-resolution structure of yeast E3 from *Saccharomyces oviformis* has been reported (17). To elucidate the reason for the different structural properties mentioned

<sup>1</sup> This work was supported in part by Grants-in-Aid for Scientific Research on Priority Areas (No. 08214203, 07230224, and 07250205) from the Ministry of Education, Science, Sports and Culture of Japan, and by the Sakabe project of TARA (Tsukuba Advanced Research Alliance), University of Tsukuba.

<sup>2</sup> To whom correspondence should be addressed. Phone: +81-45-924-5709, Fax: +81-45-924-5748, E-mail: atakenak@bio.titech.ac.jp

Abbreviations: OGDC, 2-oxoglutarate dehydrogenase complex; PDC, pyruvate dehydrogenase complex; BCDC, branched-chain 2-oxoacid dehydrogenase complex; E1, pyruvate dehydrogenase, 2-oxoglutarate dehydrogenase, or branched-chain 2-oxoacid dehydrogenase; E2, acetyltransferase, succinyltransferase, or acyltransferase; E3, dihydrolipoamide(lipoamide) dehydrogenase; FAD, flavin adenine dinucleotide; E1BD, E1 binding domain; E3BD, E3 binding domain.

<sup>3</sup> Each complex consists of the following components, PDC (E1, pyruvate dehydrogenase; E2, acetyltransferase; E3, lipoamide dehydrogenase), OGDC (E1, 2-oxoglutarate dehydrogenase; E2, succinyltransferase; E3, lipoamide dehydrogenase), and BCDC (E1, branched-chain 2-oxo acid dehydrogenase; E2, acyltransferase; E3, lipoamide dehydrogenase).

<sup>4</sup> In PDC of procaryotic Gram-positive bacteria, E3 binds E3BD of E2 even in the core with 532 symmetry.

above in eucaryotic E3s, the X-ray structure of E3, lipoamide dehydrogenase from *Saccharomyces cerevisiae* has been determined at 2.7 Å (partially at 2.4 Å) resolution. In this paper we discuss the regions of E3 involved in protein-protein interaction on the basis of the highly conserved tertiary structure.

### STRUCTURE DETERMINATION

As described in the previous paper (18), crystals of the newly purified enzyme exhibited X-ray diffraction beyond 2.5 Å resolution. For structure determination, all the observed data were used, but their coverage decreased in the outer shell over 2.68 Å resolution from 83.5% to less than 50% (see Table I). The initial phases (18) derived preliminarily from molecular replacement (18, 19) were further improved by non-crystallographic symmetry aver-

TABLE I. Crystal data and refinement statistics for yeast lipoamide dehydrogenase.

Space group	$P2_12_12_1$
Cell constants (Å)	
<i>a</i>	97.1
<i>b</i>	158.7
<i>c</i>	67.9
<i>Z</i> <sup>a</sup>	2
Limiting resolution (Å)	2.4
Observed reflections	97,677
Independent reflections <sup>b</sup>	33,372
<i>R</i> <sub>merge</sub> (%)	6.7
Completeness (%)	97.4 (100-2.87 Å resolution shell) 83.5 (2.87-2.68 Å resolution shell) 42.7 (2.68-2.40 Å resolution shell)
Non-hydrogen protein atoms	7,356
Solvent molecules	73
Reflections used for refinement	25,458
Resolution range (Å)	10-2.4
<i>R</i> -factor (%)	20.2
<i>R</i> <sub>free</sub> <sup>c</sup> (%)	26.2
R.m.s. standard deviation	
bond length (Å)	0.009
bond angles (°)	2.53
improper angles (°)	0.763
Average coordinate error (Å)	0.35

<sup>a</sup>Number of subunits in the asymmetric unit. <sup>b</sup> $I > 4\sigma$ . <sup>c</sup>Calculated using the 10% fraction of the whole reflection data which were not used for refinement.

aging, solvent flattening and histogram matching techniques with the program SQUASH (20). The molecular structure was constructed by replacing, inserting, and deleting amino acid residues in the initial polyalanine model for molecular replacement, their conformations being accommodated into electron density maps using the program O (21). After four rounds of density modification, all the inserted amino acid residues and FAD molecules were clearly located. The atomic coordinates were refined in reciprocal space using the program X-PLOR (22) and the structure model was adjusted in real space with the program O (21), alternately. For the first several rounds of positional refinements, the two subunits of the dimeric enzyme were constrained with a non-crystallographic two-fold symmetry. After stimulated annealing refinement with the temperature decreasing from 3,000 to 300 K in steps of 25 K, the structure was further refined positionally without the non-crystallographic symmetry constraint, and then the individual temperature factors of all atoms were adjusted isotropically. Seventy-three peaks in total with greater than  $3\sigma$  level in a difference electron density map and with a distance less than 3.4 Å away from the protein molecule were assigned as water molecules by taking hydrogen bond geometries into consideration, and they were added in the refinement. All residues and FADs were confirmed visually by their omit maps. During the course of refinements, the protein structure was verified using the program PROCHECK (23). The progress of refinement was monitored in terms of the free *R* value (24).

### RESULTS

The final structure showed an *R*-factor of 0.202 for 25,458 reflections with  $|F_o| > 4\sigma$  in the resolution range of 10-2.4 Å (*R*<sub>free</sub> = 0.26 for 10% of the data). The quality of the final  $2F_o - F_c$  map is shown in Fig. 1. The final structure has a small r.m.s. deviation of 0.009 Å in bond lengths and of 2.5° in bond angles from the ideal values. No residues lie in disallowed Ramachandran regions, as can be seen in Fig. 2. Crystal data, data collection and structure determination statistics are summarized in Table I.

As shown in Fig. 3, the yeast E3 is a dimeric enzyme composed of two identical subunits each with a molecular weight of 52,300 (478 amino acid residues). The two

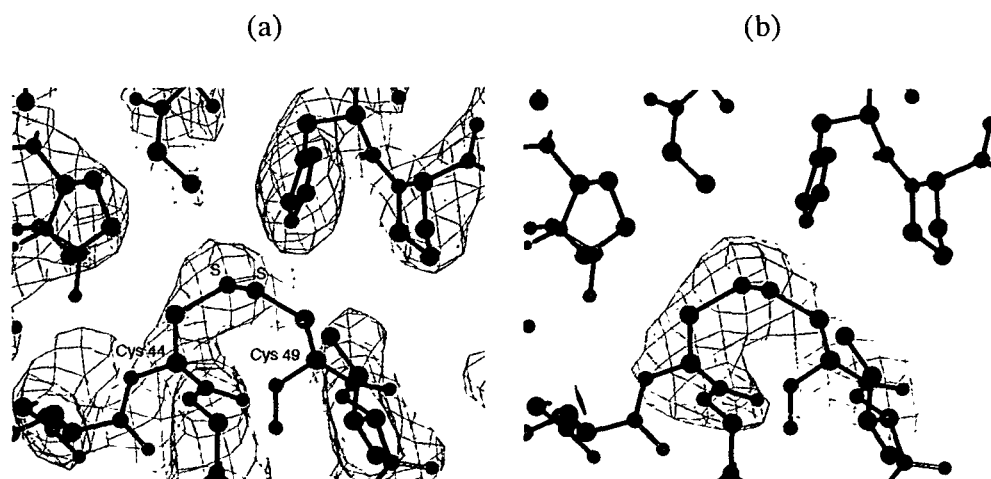


Fig. 1. The final  $2F_o - F_c$  electron density map (a) around Cys44 and Cys49, contoured at the  $1.0\sigma$  level, and its  $F_o - F_c$  omit map (b) calculated without them, contoured at the  $2.5\sigma$  level.

subunits are related by a pseudo twofold symmetry with the r.m.s. displacement of 0.56 Å for  $C_\alpha$  atoms. The individual  $C_\alpha$  displacements larger than  $3\sigma$  [ $\sigma$  is estimated to be 0.35 Å from a Luzzati plot (26)] are locally found in the loop regions with residues 70–71, 133–140, 267–268, and 351–353, which are all located on the molecular surface

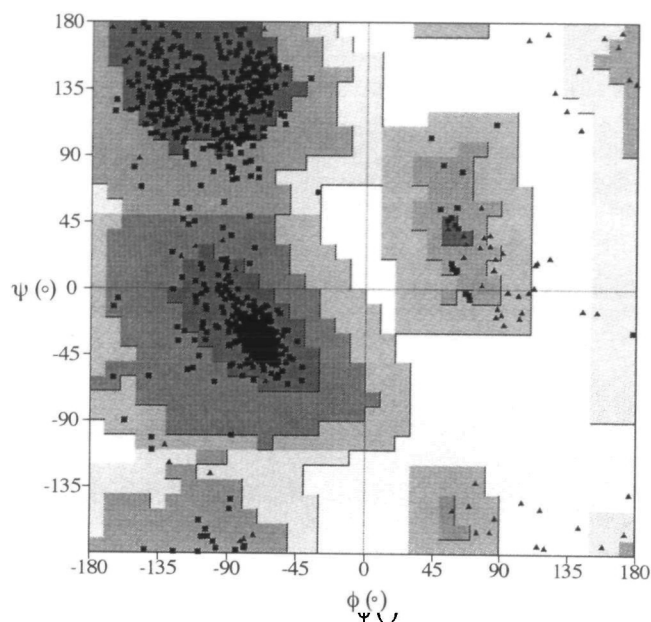


Fig. 2. A Ramachandran plot of the final structure, produced by PROCHECK (23). ▲ and ■ indicate glycine and non-glycine residues, respectively.

(see Fig. 4). Thus, the two subunits have essentially the same structure despite local differences due to crystal packing. Each subunit contains 13  $\alpha$ -helices and 24  $\beta$ -strands which constitute 31 and 27% of the whole residues, respectively. The subunit is divided into the four domains as already defined by Thieme *et al.* (27) for glutathione reductase: the FAD domain (residues 1 to 153, 3  $\alpha$ -helices, and 9  $\beta$ -strands), the NADH domain (residues 154–287, 3  $\alpha$ -helices, and 9  $\beta$ -strands), the central domain (residues 288–356, 2  $\alpha$ -helices, and 1  $\beta$ -strand), and the interface domain (residues 357–478, 5  $\alpha$ -helices, and 5  $\beta$ -strands). A disulfide bond is formed between Cys44 and Cys49, which are essential for the dehydrogenase activity.

The solvent accessible surface was calculated with the program SURFACE in CCP4 (28). About 3,900 Å<sup>2</sup> (16%) of the subunit surface is buried through dimerization. The region involved in the subunit-subunit interaction is constituted from the FAD domain and the interface domain. The residues 61–83 in the FAD domain come into contact with those related by a pseudo twofold symmetry, in which residues 74–82 form a bent anti-parallel  $\beta$ -sheet with the corresponding residues 74'–82' of the counter subunit, as shown in the top and side views in Fig. 3. In addition, the remaining hydrophobic residues (Ile74, Val76, Ile80, and Ile82 in the  $\beta$ -strand and Leu61, Phe62, and Met65 in the adjacent  $\alpha$ -helix) also interact with the corresponding residues of the other subunit. In the interface domain,  $\alpha$ -helices and loops involving residues 397–477 interact with the other subunit through hydrogen bonds and hydrophobic interactions. The two active sites of the enzyme are located separately at the interface of two subunits and each consists of FAD, Cys44, and Cys49 from one subunit and

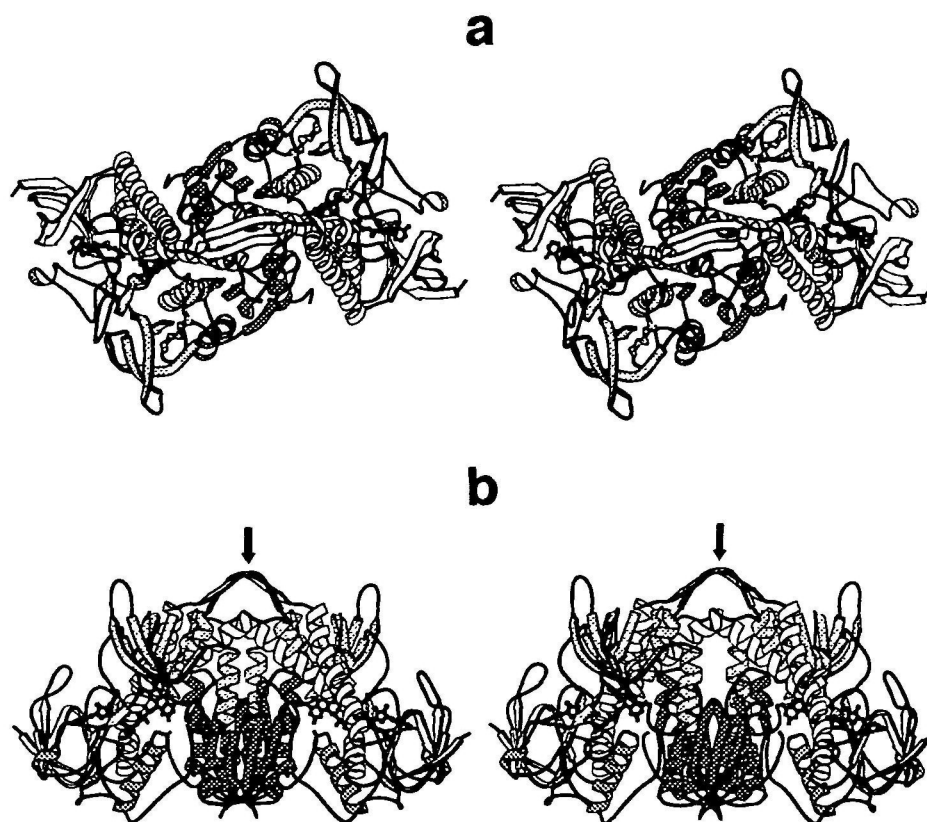


Fig. 3. A stereo diagram of a ribbon drawing of the dimeric yeast lipoamide dehydrogenase (a) viewed down the molecular twofold axis and (b) viewed perpendicular to it. The FAD molecules are drawn as ball-and-stick models. An arrow indicates the intersubunit  $\beta$ -sheet (residues 74–82). The four domains (FAD, NADH, central, and interface domains) are depicted with no shade and with shades of light gray, gray, and dark gray, respectively. The figures were produced with the program MOLSCRIPT (25).

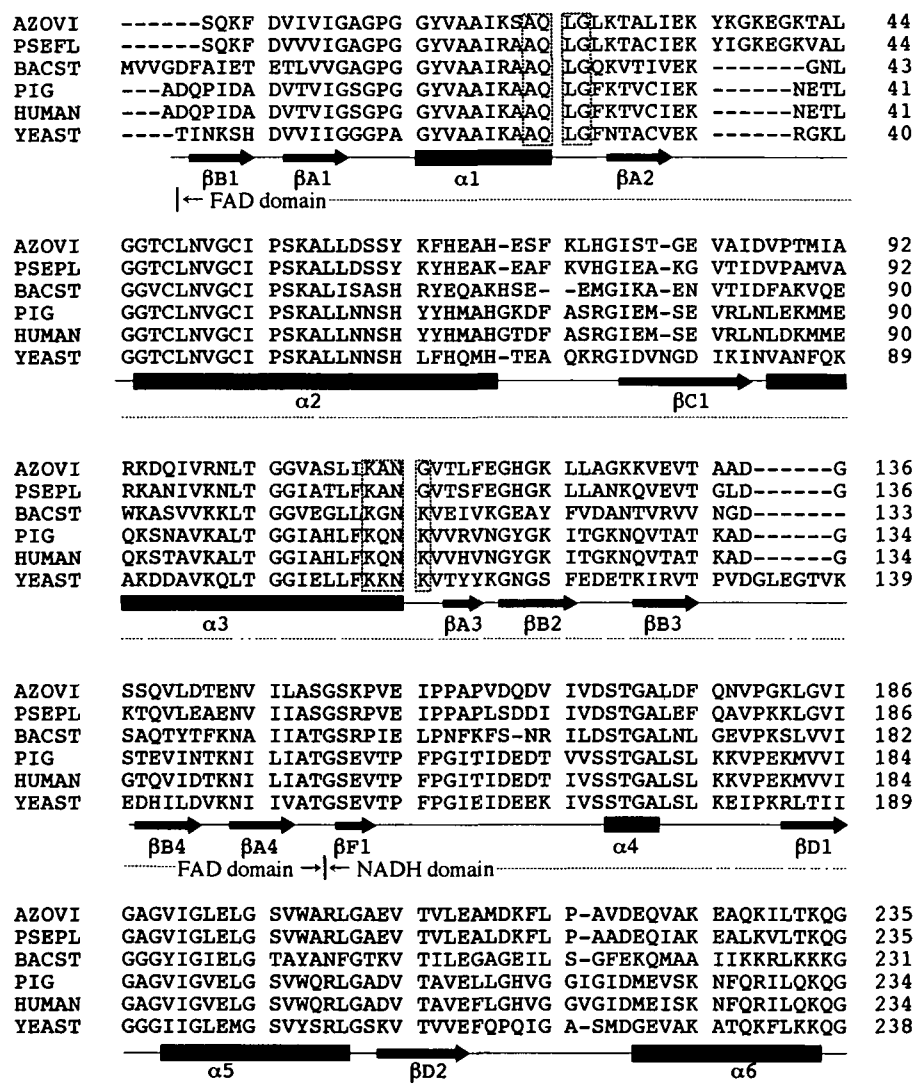


Fig. 4. (Continued on the next page)

His457' from the other subunit (see Fig. 6).

#### DISCUSSION

It is interesting to compare the present eucaryotic E3 structure with those of procaryotes, *A. vinelandii* (14), *P. putida* (15), *P. fluorescens* (16), and *B. stearothermophilus* (12). The new  $\beta$ -sheet found in yeast E3 is missing in the other E3s, except *P. fluorescens* E3. Figure 5 shows their structures superimposed on the corresponding  $C_{\alpha}$  atoms with the closest tertiary structure. Large differences occur only in the loop regions containing insertion or deletion of amino acids and in the new  $\beta$ -strand ( $\beta C1$ ), as shown in Fig. 4. The r.m.s. deviation of  $C_{\alpha}$  atoms without those residues is 0.9 Å among the molecules. It is thus concluded that the yeast E3 has the same basic tertiary structure as the procaryotic E3s, even though the amino acid sequence identity is rather low, namely 42–44%. Although the *P. putida* E3 (15) is a component of BCDC (of which the architecture is not yet known) and has an even lower sequence identity with the yeast E3 (35%), the tertiary structure is very similar to those of the other E3s.

All E3s have two catalytic sites, each of which is formed with the flavin moiety of FAD and two cysteine residues from one subunit and a histidine residue from the other subunit. Their r.m.s. displacement is only 0.3 Å, as shown in Fig. 6. The active site is highly conserved among the eucaryotic and the procaryotic E3s even though the amino acid identity is less than 50%. As pointed out in the structure of E3 from *A. vinelandii* (14), for the catalytic reaction, a lipoamide group of E2 must enter the active site toward the Cys44 and Cys49 side of the flavin plane, because the nicotine moiety of  $NAD^{+}$  interacts on the other side (15). In this situation, the lipoyl domain of E2 will approach the active site formed between the FAD and the interface domains, from one side, i.e. from the front side toward the right flavin moiety in Fig. 3 (b).

In eucaryotic PDC, E3 binds E3BD of protein X but not E2(acetyltransferase) which has an E1BD, while, in eucaryotic OGDC, E3 binds E3BD of E2(succinyltransferase) directly. The E3 binding site of E2 has been proposed based on an X-ray analysis of E3BD of E2(acetyltransferase) from *B. stearothermophilus* (12) complexed with E3. The essential basic amino acids, arginine and lysine (in a box in

AZOVI	LKILLGARVT	GTEVK-NKQV	-TVKFVDAEG	EKSQAF--DK	LIVAVGRRPV	281
PSEPL	LNIRLGARVT	ASEVK-KKQV	-TVTFTDANG	EQKETF--DK	LIVAVGRRPV	281
BACST	VEVVTNALAK	GAEER-EDGV	-TVTYEANGE	TKTIDA--DY	VLVTVGRRPN	277
PIG	FKFKLNTRVI	GATKKS D GNI	-DVSIEAASG	GKAEVITCDV	LLVCIGRRPF	283
HUMAN	FKFKLNTRVT	GATKKS D GKI	-DVSIEAASG	GKAEVITCDV	LLVCIGRRPF	283
YEAST	LDFKLS TKVI	SAKRND D KNV	VEIVVEDTKT	NKQENLEAEV	LLVAVGRRPY	288
	----- NADH domain ----->					
AZOVI	TFDLLAADSG	VTLDERGFIY	VDDYCATSVP	GVYAIGDVVR	GAMLAHKASE	331
PSEPL	TFDLLAADSG	VTLDERGFIY	VDDHCRTSVP	GVFAIGDVVR	GAMLAHKASE	331
BACST	TDELGLEQIG	IKMTNRGLIE	VDQQCRTSVP	NIFAIGDIVV	GPALAHKASY	327
PIG	TQNLGLEELG	IELDPRGRIP	VNTRFQTKIP	NIYAIGDVVA	GPMLAHKAED	333
HUMAN	TKNLGLEELG	IELDPRGRIP	VNTRFQTKIP	NIYAIGDVVA	GPMLAHKAED	333
YEAST	IAGLGAEKIG	LEVDKRGRLV	IDDQFNSKFP	HIKVVGDVTF	GPMLAHKAEE	338
	----- Central domain ----->					
AZOVI	EGVVVAERIA	GHKAMNYDL	IPAVIYTHPE	IAGVGKTEQA	LKAEGVAINV	381
PSEPL	EGVMVAERIA	GHKAMNYDL	IPSVIYTHPE	IAVVGKTEQT	LKAEGVEVNV	381
BACST	EGKVAEAEIA	GHPSAVDYVA	IPAVVFS D PE	CASVGYFEQQ	AKDEGIDVIA	377
PIG	EGIIICVEGMA	GGAVHIDYNC	VPSVIYTHPE	VAVVGKSEEQ	LKEEGIEYKV	383
HUMAN	EGIIICVEGMA	GGAVHIDYNC	VPSVIYTHPE	VAVVGKSEEQ	LKEEGIEYKV	383
YEAST	EGIAAVEMLK	TGHGHVNYNN	IPSVMYSHPE	VAVVGKTEEQ	LKEAGIDYKI	388
	----- Central domain -----> Interface domain ----->					
AZOVI	GVFPFAASGR	AMAANDTAGF	VKVIADAKTD	RVLGVHVIGP	SAAELVQOGA	431
PSEPL	GVFPFAASGR	AMAANDTTGL	VKVIADAKTD	RVLGVHVIGP	SAAELVQOGA	431
BACST	AKFPFAANGR	ALALNDTDGF	LKLVVRKEDG	VIIGAQIIGP	NASDMIAELG	427
PIG	GVFPFAANSR	AKTNADTDGM	VKILGQKSTD	RVLGAHIIGP	GAGEMINEAA	433
HUMAN	GVFPFAANSR	AKTNADTDGM	VKILGQKSTD	RVLGAHILGP	GAGEMVNEAA	433
YEAST	GVFPFAANSR	AKTNQDTEGF	VKILIDSKTE	RILGAHIIGP	NAGEMIAEAG	438
AZOVI	IAMEFGTSAE	DLGQMVFAHP	ALSEALHEAA	LAVSGHAIHV	ANRKK----	476
PSEPL	IGMEFGTSAE	DLGQMVFSHP	TLSEALHEAA	LAVNGHAIHI	ANRKKR----	477
BACST	LAIEAGMTAE	DIAITIH AHP	TLGEIAMEAA	EVALGTP IHI	ITK-----	470
PIG	LALAYGASCE	DIAFVCHAHP	TLSEAFKEAN	LAASFGKAIN	F-----	474
HUMAN	LALAYGASCE	DIAFVCHAHP	TLSEAFKEAN	LAASFGKIN	F-----	474
YEAST	LALAYGASAE	DVARVCHAHP	TLSEAFKEAN	MAAYD-KATH	C-----	478
	----- Interface domain ----->					



Fig. 7) pointed out by Mande *et al.* (12), are also found in the corresponding site of E3BD of yeast OGDC E2 (succinyltransferase), but they are replaced with neutral or hydrophobic ones in the E3BD of the yeast protein X.<sup>5</sup> Therefore these differences suggest that the yeast E3 is

<sup>5</sup> Recently the amino acid sequence of the human protein X has been reported (6), and in this molecule the positive charges in this region are reduced.

Fig. 4. Comparison of primary structures among procaryotic and eucaryotic E3s. The sequence data were taken from GenBank (29). Key to sequence origins: AZOVI, *Azotobacter vinelandii*; PSEFL, *Pseudomonas fluorescens*; BACST, *Bacillus stearothermophilus*. The bottom line shows the four domains of the yeast E3, together with the secondary structures. Rectangles and arrows indicate  $\alpha$ -helices and  $\beta$ -strands, respectively. Amino acids in boxes surrounded by solid lines are those located in the conserved negative potential region ① (see Fig. 8) around the 2-fold axis for E2 binding. The outlined letters indicate the essential acidic amino acids for binding with E3BD of E2. Amino acids, found in the region whose potentials characteristically differ between yeast E3 and procaryotic E3 (surrounded by dotted line in Fig. 8) are enclosed in the dot-lined boxes. Amino acids in shaded boxes are those found in region ② of Fig. 8. Bold letters indicate amino acids replaced in eucaryotic E3s with basic amino acids from neutral ones.

Fig. 5. A stereo diagram of four lipamide dehydrogenase structures. They are superimposed between the corresponding C $\alpha$  atoms of the dimers, but only the subunits are shown for clarity. The C $\alpha$  atoms are traced with thick lines for yeast, thin lines for *Azotobacter vinelandii*, broken lines for *Pseudomonas fluorescens*, dotted lines for *Bacillus stearothermophilus*.

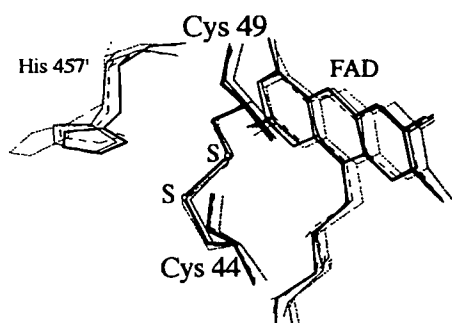


Fig. 7. Amino acid sequences of the E3 binding region of E2 in procaryotic PDC and in procaryotic and eucaryotic OGDC, taken from GenBank (29). Key to sequence origins: AZOVI, *Azotobacter vinelandii*; ECOLI, *Escherichia coli*; BACSU, *Bacillus subtilis*; BACST, *Bacillus stearothermophilus*. The basic amino acids proposed to be the E3 binding site (28) are in a box. The bottom line shows the amino acid sequence in the corresponding region of yeast protein X. The basic amino acids are replaced with neutral or hydrophobic ones. (Although the amino acid sequence in the corresponding region of PDC E2 is similar to that of E3BD of OGDC E2 (12), it is omitted in the figure due to the fact that PDC E3 binds protein X but not E2.)

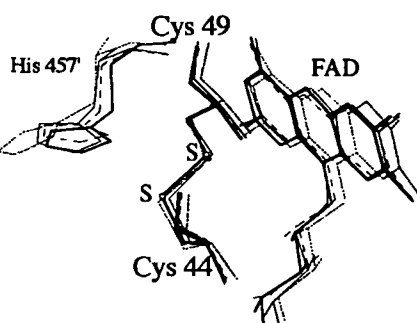


Fig. 6. A stereo view of the active sites superimposed among four lipoamide dehydrogenases from yeast with thick lines, *Azotobacter vinelandii* with thin lines, *Pseudomonas fluorescens* with broken lines, and *Bacillus stearothermophilus* with dotted lines. The residue numbers are for yeast E3.

AZOVI	E2 (OGDC)	-LSPAARKIAE	E-N---AIAA	DSITGTGKGG	RVTKEDAVA-
ECOLI	E2 (OGDC)	-LSPAIRRLLA	E-H---NLDA	SAIKGTGVGG	RLTREDVEK-
BACSU	E2 (OGDC)	-ASPSARKLAR	E-K--GIDL	QVPTG-DPLG	RVRKQDVEA-
HUMAN	E2 (OGDC)	-QPPSGKPVSA	V-K---PTVA	-----	-----
RAT	E2 (OGDC)	-QPPSKPVSA	I-K---PTAA	-----	-----
YEAST	E2 (OGDC)	-KKPLQRKIQ	NQK---RTDQ	PKK-----	-----
AZOVI	E2 (PDC)	-AGPAVRQLAR	E-F---GVEL	AAINSTGPRG	RILKEDVQA-
ECOLI	E2 (PDC)	-ATPLIRRLAR	E-F---GVNL	AKVKGTGRK	RILREDVQA-
BACST	E2 (PDC)	-AMPSVRKYAR	E-K---GVDI	RLVQGTGKNG	RVLKEDIDA-
BACSU	E2 (PDC)	-AMPSVRKYAR	E-K---GVDI	RKVTGSGNNG	RVLKEDIDS-
YEAST	X (PDC)	-LLPSVSLLLA	ENNISKQKAL	KEIAPSGSNG	RLKGDVLA-

bound to two different E3BDs of protein X and E2. On the other hand, the procaryotic E3 is bound to only the similar E3BDs of E2s in PDC and OGDC.

To investigate the structural properties of the yeast E3, an electrostatic potential surface was calculated and compared with those of the procaryotic E3s. The most remarkable feature is the large negative region ① localized at the bottom around the twofold axis of the dimeric enzyme, as shown in Fig. 8. This negative region is commonly found in all the E3s, and is just the same as the proposed binding site of E2 (12). In Fig. 4, the amino acid residues involved in this region are localized in four boxes. In particular, Glu442, Glu448, and Asp449 participate to create the negative potential which can facilitate binding with E3BD of E2 in yeast OGDC, because, as seen in Fig. 7, the E3 binding site has basic amino acids similar to those of *B. stearothermophilus* PDC. Therefore, this region is electrostatically conserved between the procaryotic and the eucaryotic yeast E3s as regards the binding site of E2.

Further comparison of electrostatic potentials showed an adjacent region surrounded with dotted lines in Fig. 8, whose potentials characteristically differ between the yeast E3 and the procaryotic E3s. The amino acids in this region are shown in dot-lined boxes in Fig. 4. This region is still negative in the procaryotic E3s as an extension from region ①. The lower part of the dot-lined region (surrounded with a full line as region ② in Fig. 8; the amino acids are shown in shaded boxes in Fig. 4) belongs to the interface domain distant from the active site. Several residues in region ② of yeast E3 definitely differ in charge or in polarity from those of the procaryotic E3s. In particular, the four basic residues, Lys387, Arg452, Lys465, and Lys474, in the yeast E3 (bold letters in Fig. 4) neutralize the negative field caused by Glu462 and Glu466. These changes are reflected in the molecular surface potential as if to differentiate it

from the negative potential of the procaryotic E3. In other eucaryotic E3s, the same or similar amino acid changes occur (Fig. 4), suggesting a common feature of their electrostatic potentials conserved in eucaryotes. On the other hand, the amino acids of protein X, which correspond to those of E3BD on E2, are completely different, having a rather hydrophobic characters. If they participate in E3 binding, the binding site on E3 must also be hydrophobic. Such a region can be found adjacent to ②. Therefore region ② may be neutralized to facilitate the binding. It might thus be concluded that the region adjacent to ② is a possible binding site of protein X, because it is near the E2 binding site but distant from the other binding sites for the substrate and the coenzyme. As a result, the yeast E3 will have two binding regions for E2 of OGDC and for protein X of PDC. As discussed above, the tertiary structures of E3s are highly conserved between eucaryotes and procaryotes. In the evolutionary process, the molecular surface of eucaryotic E3 might have changed to adapt to the architecture of PDC after introduction of protein X.

We are grateful to N. Sakabe and N. Watanabe for facilities and help during data collection at the Photon Factory (Tsukuba). We thank J.C. Thierry for helpful discussions and comments on this study.

#### REFERENCES

- Reed, L.J. (1974) Multienzyme complexes. *Acc. Chem. Res.* **7**, 701-729
- Mattevi, A., de Kok, A., and Perham, R.N. (1992) The pyruvate dehydrogenase multienzyme complex. *Curr. Opin. Struct. Biol.* **2**, 877-887
- Perham, R.N. (1991) Domains, motifs, and linkers in 2-oxo acid dehydrogenase multienzyme complexes: A paradigm in the design of a multifunctional protein. *Biochemistry* **30**, 8501-8512
- Henderson, C.E., Perham, R.N., and Finch, J.T. (1979) Structure and symmetry of *Bacillus stearothermophilus* pyruvate dehy-

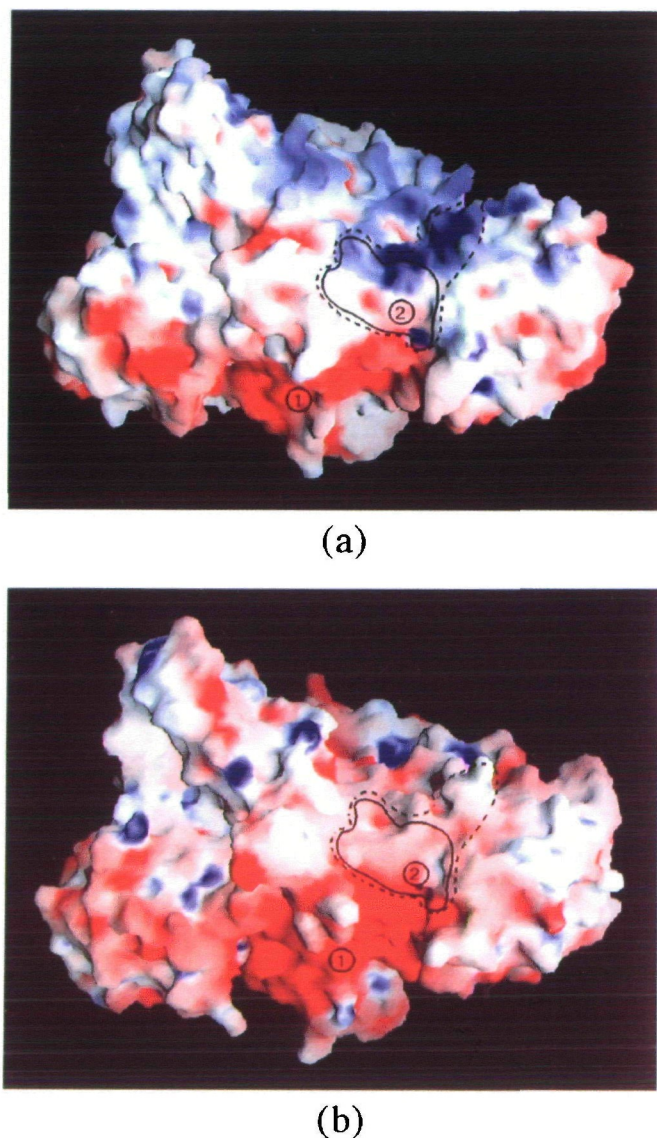


Fig. 8. Electrostatic potential surfaces (positive in blue and negative in red) on the bottom side around the pseudo twofold axis, (a) for yeast E3 and (b) for *Azotobacter vinelandii* E3. The central negative region ① has been proposed as the E3BD of E2 (12). A region, definitely changed in electrostatic potential between the yeast E3 (a) and the prokaryotic E3 (b), is surrounded with dotted line. The surrounded region ② is proposed as a candidate for facilitating the protein X binding (see the text).

drogenase multienzyme complex and implications for eucaryote evolution. *Cell* 17, 85–93

5. Behal, R.H., Browning, K.S., Hall, T.B., and Reed, L.J. (1989) Cloning and nucleotide sequence of the gene for protein X from *Saccharomyces cerevisiae*. *Proc. Natl. Acad. Sci. USA* 86, 8732–8736
6. Marcucci, O. and Lindsay, J.G. (1985) Component X. An immunologically distinct polypeptide associated with mammalian pyruvate dehydrogenase multi-enzyme complex. *Eur. J. Biochem.* 149, 641–648
7. Harris, R.A., Bowker-Kinley, M.M., Wu, P., Jeng, J., and Popov, K.M. (1997) Dihydrolipoamide dehydrogenase-binding protein of the human pyruvate dehydrogenase complex. *J. Biol. Chem.* 272, 19746–19751
8. Gopalakrishnan, S., Rahmatullah, M., Radke, G.A., Powers-Greenwood, S., and Roche, T.E. (1989) Role of protein X in the function of the mammalian pyruvate dehydrogenase complex. *Biochem. Biophys. Res. Commun.* 160, 715–721
9. Robien, M.A., Clore, C.M., Omichinski, J.G., Perham, R.N., Appella, E., Sakaguchi, K., and Gronenborn, A. (1992) Three-dimensional solution structure of the E3-binding domain of the dihydrolipoamide succinyltransferase core from the 2-oxoglutarate dehydrogenase multienzyme complex of *Escherichia coli*. *Biochemistry* 31, 3463–3471
10. Dardel, F., Davis, A.L., Laue, E.D., and Perham, R.N. (1993) Three-dimensional structure of the lipoyl domain from *Bacillus stearothermophilus* pyruvate dehydrogenase multienzyme complex. *J. Mol. Biol.* 229, 1037–1048
11. Green, J.D., Laue, E.D., Perham, R.N., Ali, S.T., and Guest, J.R. (1995) Three-dimensional structure of a lipoyl domain from the dihydrolipoamide acetyltransferase component of the pyruvate dehydrogenase multienzyme complex of *Escherichia coli*. *J. Mol. Biol.* 248, 328–343
12. Mande, S.S., Sarfaty, S., Allen, M.D., Perham, R.N., and Hol, W.G.J. (1996) Protein-protein interactions in the pyruvate dehydrogenase multienzyme complex: dihydrolipoamide dehydrogenase complexed with the binding domain of dihydrolipoamide acetyltransferase. *Structure* 4, 277–286
13. Mattevi, A., Obmolova, G., Schulze, E., Kalk, K.H., Westphal, A.H., Kok, A., and Hol, W.G.J. (1992) Atomic structure of the cubic core of the pyruvate dehydrogenase multienzyme complex. *Science* 255, 1544–1550
14. Mattevi, A., Schierbeek, A.J., and Hol, W.G.J. (1991) Refined crystal structure of lipoamide dehydrogenase from *Azotobacter vinelandii* at 2.2 Å resolution. *J. Mol. Biol.* 220, 975–994
15. Mattevi, A., Obmolova, G., Sokatch, J.R., Betzel, C., and Hol, W.G.J. (1992) The refined crystal structure of *Pseudomonas putida* lipoamide dehydrogenase complexed with NAD<sup>+</sup> at 2.45 Å resolution. *Proteins* 13, 336–351
16. Mattevi, A., Obmolova, G., Kalk, K.H., van Berkel, W.J.H., and Hol, W.G.J. (1993) Three-dimensional structure of lipoamide dehydrogenase from *Pseudomonas fluorescens* at 2.8 Å resolution. *J. Mol. Biol.* 230, 1200–1215
17. Takenaka, A., Kizawa, K., Hata, T., Sato, S., Misaka, E., Tamura, C., and Sasada, Y. (1988) X-ray study of baker's yeast lipoamide dehydrogenase at 4.5 Å resolution by molecular replacement method. *J. Biochem.* 103, 463–469
18. Toyoda, T., Sekiguchi, T., and Takenaka, A. (1997) Crystallization of eukaryotic E3, lipoamide dehydrogenase from yeast, for exhibiting X-ray diffractions beyond 2.5 Å resolution and preliminary structure analysis. *J. Biochem.* 121, 1–4
19. Navaza, J. (1994) AMoRe: an automated package for molecular replacement. *Acta Cryst.* A50, 157–163
20. Zhang, K.Y.J. (1993) SQUASH—Combining constraints for macromolecular phase refinement and extension. *Acta Cryst.* D49, 213–222
21. Jones, T.A., Zou, J.Y., Cowan, S.W., and Kjeldgaard, M. (1991) Improved methods for building protein models in electron density maps and the location of errors in these models. *Acta Cryst.* A47, 110–119
22. Brünger, A.T. (1992) *X-PLOR. Version 3.1. A System for X-Ray Crystallography and NMR*, Yale University Press, New Haven, CT
23. PROCHECK in Collaborative Computational Project, Number 4 (1994) The CCP4 suite: programs for protein crystallography. *Acta Cryst.* D50, 760–763
24. Brünger, A.T. (1992) Free-R value: a novel statistical quantity for assessing the accuracy of crystal structures. *Nature* 355, 472–475
25. Carson, M. (1991) Ribbons 2.0. *J. Appl. Cryst.* 24, 958–961
26. Luzzati, P.V. (1952) Traitement statistique des erreurs dans la détermination des structures cristallines. *Acta Cryst.* 5, 802–810
27. Thieme, R., Pai, E.F., Schirmer, R.H., and Schulz, G.E. (1981) Three-dimensional structure of glutathione reductase at 2 Å resolution. *J. Mol. Biol.* 152, 763–782
28. Collaborative Computational Project, Number 4 (1994) The CCP4 suite: programs for protein crystallography. *Acta Cryst.* D50, 760–763
29. Benson, D.A., Boguski, M., Lipman, D. J., and Ostell, J. (1994) GenBank. *Nucleic Acids Res.* 22, 3441–3444